Proceedings of the XVII ECSMGE-2019
Geotechnical Engineering foundation of the future
ISBN 978-9935-9436-1-3

doi: 10.32075/17ECSMGE-2019-0042

XVII European Conference
ECSMGE 2019
Reykjavik
on Soil Mechanics
and Geotechnical Engineering

Evolution of pore water pressures at the base of rapid fine-grained material flows

Evolution des pressions interstitielles à la base des écoulements rapides de matériaux fins

Francesco Federico
Associate Professor of Geotechnics, University of Rome Tor Vergata (Rome, Italy)
Chiara Cesali
Ph. D. Student in Geotechnical Engineering, University of Rome Tor Vergata (Rome, Italy)

ABSTRACT: The speed evolution and runout length of rapid fine-grained material flows (e.g. mudflows, quick clays) are analytically modelled by taking into account the evolution of the basal pore water pressures according to consolidation process typically affecting the involved materials, as well as their possible increments initially generated due to several phenomena (e.g. earthquakes) and during the motion due to the slope curvature coupled to undrained and oedometric conditions.
The mass variations due to possible erosion or deposition processes occurring along the motion are also considered. The governing ordinary differential equation has been numerically solved. The role played by the main parameters on the kinematics of the material flows and the range of their admissible values are evaluated.
The analysis and interpretation of measurements (lab and in situ) of sliding rate, runout length and pore water pressures are finally developed and carried out.

RÉSUMÉ: L'évolution de la vitesse et la longueur du ruissellement des flux de matériaux rapides à grains fins (e.g. des coulées de boue, des argiles rapides) sont modélisés de manière analytique en prenant en compte l'évolution des pressions d'eau dans les pores de la base selon un processus de consolidation affectant généralement les matériaux en cause, ainsi que leurs incréments possibles générés initialement en raison de plusieurs phénomènes (e.g. des tremblements de terre) et pendant le mouvement en raison de la courbure de la pente couplée à des conditions non drainées et oedométriques. De plus, les variations de masse dues aux processus possibles d'érosion ou de dépôt se produisant le long du mouvement sont également prises en compte.
L'équation différentielle ordinaire qui régit a été résolue analytiquement et numériquement. Le rôle joué par les principaux paramètres de la cinématique des écoulements rapides de matériaux fins et la plage de leurs valeurs admissibles sont évalués.
L'analyse et l'interprétation des mesures du taux de glissement, de la longueur du ruissellement et des pressions interstitielles sont finalement développées et réalisées.

Keywords: Pore Water Pressure Evolution, Consolidation, Slope Curvature, Mass change.

1 INTRODUCTION

The triggering mechanisms and successive sliding of fine-grained material flows considerably depend on the excess pore water pressures (Hutchinson and Bhandari 1971), followed by a consolidation process.

The excess pore water pressures (*pwp*) can be generated by *(i)* shear strains induced by an earthquake; *(ii)* deposition under own weight of granular masses, initially liquefied (Federico and Cesali 2017); *(iii)* rapid accumulation of rainwater in soil layers affected by a low permeability; *(iv)* seepage flow in boundary materials; *(v)* redistribution of the total stresses caused by internal mechanisms of failure or reactivation (Comegna and Picarelli 2005); *(vi)* compressive deformation of flow body associated with local variation in the slope of the sliding surface or due to a centrifugal force acting along a curvilinear path (Siviglia and Cantelli 2005); *(vii)* consolidation processes under oedometric and undrained conditions (Lambe and Whitman 1969). The considerable shear strength reduction, due to the generation of *pwp* excess, is often the main reason of slope failures and high mobility of material volumes, even along very gentle slopes; high *pwp* can also induce the partial or complete liquefaction of the soil (Iverson et al. 1997).

Conversely, the consolidation process of fine-grained materials during the motion may progressively reduce the *pwp;* the corresponding increase in the shear strength reduces the travelled distance.

Generally, the kinematics of granular flows can be also remarkably influenced by mass variations ($\dot{m}$) due to erosion or deposition processes; erosion phenomena may affect the channel bed or the erodible lateral surfaces (Hungr 2004). Typically, the erosion phenomenon (mass rate $\dot{m} > 0$) mainly occurs at high elevation, due to the high slope (up to critical erosion angle β_e) and the great travel speed, causing strongly increments of the involved volume; the deposition ($\dot{m} < 0$) is caused by the slowdown due in turn to the reduction of slope, or along a counterslope.

To study the effects of (excess) *pwp* evolution on the kinematics of fine – grained materials flows, a more general *sliding block* model is proposed.

2 PROPOSED MODEL

Geometry. The motion of a fine-grained material block of thickness $\bar{h}$ and length b (Fig. 1, 1 m length along the direction orthogonal to the slope, $\Omega = b \cdot 1$) is considered. The slope α of the sliding surface may generally decrease or increase along its curved path (s = curvilinear abscissa, r = curvature radius).

The sliding surface (*s.s.*) can be schematized through: *a*) an arc of circumference; *b*) two planar surfaces linked by an arc of circumference ($1/r \neq 0$ starting by $s = 0$); *c*) two planar surfaces, i.e. $r \rightarrow \infty$.

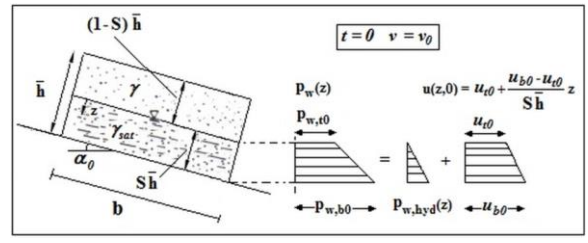

Figure 1. Geometry of the sliding mass and assumed initial pore water pressure distribution.

Pore water pressures. A trapezoidal initial *pwp* distribution ($p_w(z)$) within a basal layer of thickness $S\bar{h}$ (S = percentage of saturated layer ϵ [0,1]) is assumed (Fig. 1). The initial values $p_{w,t0}$ and $p_{w,b0}$ of *pwp*, at the top and the base of the saturated layer, depend on the values of hydrostatic interstitial pressure ($p_{w,hyd}(z) = \gamma_w z \cos\alpha$) and on the excess *pwp* $u(z,t)$ (z, normal to the sliding surface, directed downward, from the upper surface of the saturated soil layer, Fig. 1). The resultant U of the *pwp* at the base of the sliding mass ($p_{w,b}(t)$) is related to the sum of the basal hydrostatic

interstitial pressure ($p_{w,hyd}(z = S\bar{h}) = p_{w,b,hyd}$) and the basal excess *pwp*, at time t ($u(z = S\bar{h}, t) = u_b(t)$), multiplied by b (Fig.1):

$$U = p_{w,b}(t) \cdot b = \left[p_{w,b,hyd} + u_b(t) \right] \cdot b \qquad (1)$$

The evolution of the *pwp* excess, at the base of the sliding granular mass, is described through a simple dissipation law $u_b(t)$ (Federico and Cesali 2017):

$$u_b(t) = u_{b,0} \cdot e^{-at} \qquad (2)$$

u_{b0} (= $u(z = S\bar{h}, t = 0)$) being the initial basal *pwp excess*; *a,* a parameter related to the variables that govern the consolidation of the material. The *pwp* excess may induce negligible effective stresses in a soil mass up to liquefaction (Iverson et al. 1997; Major 2000).

The condition for liquefaction requires that the *pwp* (p_w) equals the total normal stress (σ):

$$p_w(z) = p_{w,hyd}(z) + u(z,t) = \sigma(z) = \left[\gamma\bar{h}(1-S) + \gamma_{sat} z\right]\cos\alpha \qquad (3)$$

γ being the unit weight of the unsaturated layer of thickness $(1-S)\bar{h}$; γ_{sat}, the unit weight of the saturated layer of thickness $S\bar{h}$ ($\gamma_{sat} = \gamma' + \gamma_w$, with γ' = soil effective weight; γ_w= unit weight of water).

Since the effective normal stress definition $\sigma' = \sigma - p_w$ (Terzaghi's criterion), eq. (3) implies that $\sigma' = 0$ everywhere in the soil mass. In this peculiar case, if the strength due to cohesion is also negligible, the frictional strength of the soil is zero and soils can flow quite readily, like a liquid. Furthermore, since the basal hydrostatic interstitial pressure is expressed as:

$$p_{w,hyd}(z = S\bar{h}) = p_{w,b,hyd} = \gamma_w S\bar{h} \cdot \cos\alpha \qquad (4)$$

eq. (3) (for $z = S\bar{h}$) implies that the initial basal excess *pwp* u_{b0} must be smaller than the maximum value $u_{b0,max}$:

$$u_{b0,\max} = [(1-S)\cdot\gamma + S\gamma']\cdot\bar{h}\cdot\cos\alpha \qquad (5)$$

Thus, the initial basal *pwp* u_{b0} can be expressed as follows:

$$u_{b,0} = r_{0,b} \cdot u_{b0,\max} \qquad (6)$$

$r_{0,b}$ (= $u_{b0}/u_{b0,\max}$) is defined as the ratio between the current initial *pwp* excess at the base of the granular mass and its maximum value (Hutchinson 1986); $r_{0,b} \leq 1$ must be assigned to avoid the occurrence of the *initial* soil liquefaction and to apply the proposed model.

Governing equation. The mass (m) of the sliding block may vary due to erosion/deposition processes along its motion. The governing law of motion is generalized as follows:

$$F = \frac{d[m(t)\cdot v(t)]}{dt} - w^* \frac{d[m(t)]}{dt} \qquad (7)$$

v being the velocity of the block; w^*, the velocity of the gained or lost mass. The resultant F of forces acting on the block (Fig. 2) is expressed as follows:

$$F = mg\sin\alpha - T_{\max} \qquad (8)$$

g being the gravity acceleration; α, the angle of slope of the sliding surface; T_{max}, the shear resistance force (neglecting cohesion and considering purely frictional basal resistance law):

$$T_{\max} = (N - U)\cdot\tan\varphi' \qquad (9)$$

φ' being the shear resistance angle along the basal surface; N (= $mg\cdot\cos(\alpha)$), the resultant of the total normal stresses at the base.

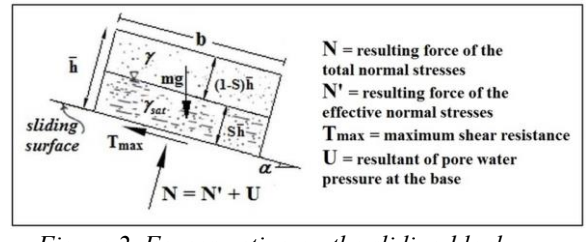

Figure 2. Forces acting on the sliding block.

The possible variation of the friction angle φ' with the velocity (Miao et al. 2014), at the base of sliding materials, is neglected.

For negligible values of the rate w^* (Van Grassen and Cruden 1990), eq. (7) can be finally rewritten as:

$$mg\,sin\alpha - \left[N - (p_{w,b,hyd} + u_b(t)\cdot b\right]\cdot tan\varphi' = m(t)\frac{dv(t)}{dt} + v(t)\frac{dm(t)}{dt} \quad (10)$$

In more general cases, the law of motion (eq. (10)) must be rewritten by taking into account the curvature ($1/r \neq 0$) of the sliding surface (Federico and Cesali, 2017) and the centripetal force ($= m\cdot \dot{s}^2/r(s) = m\cdot v^2/r(s)$) that modifies the normal resultant forces N and U and the global shear resistance force T_{max}. The reduction of the slope of the sliding surface $\alpha(s) = \alpha_0 - s/r$ (α_0, slope of the sliding surface at the beginning of the curved path) gets a decrease of the driving force ($= mgsin\alpha(s)$) and an increase of N. The current total normal force at the base of the sliding mass becomes:

$$N = mg\cos\alpha + m\frac{v^2}{r} \quad (11)$$

due to the increase $\Delta N = m\cdot v^2/r$ associated with the curvature of the sliding surface and the velocity of the sliding mass. This effect has been recently obtained through different models (Qiao et al. 2018). If the curvature assumes high values, the *pwp* doesn't vary hydrostatically (Siviglia and Cantelli 2005): the change of the direction of motion of a fluid particle (curvilinear path) induces an increase of the piezometric head and of the interstitial pressures:

$$p_w(z) = p_{w,hyd}(z) + \Delta p_{w,k}(r(z),z) \quad (12)$$

$$\text{with } \Delta p_{w,k}(r(z),z) = \gamma_w\frac{v^2}{r(z)g}z \quad (13)$$

$\Delta p_{w,k}(r(z),z)$ being the increment of pore water pressure due to the curvature of the sliding surface; $r(z) = r_b - \bar{h} + z$; r_b = curvature radius at the base of the block ($r \cong r_b$, for shallow flows). According to above equations, if $r >> \bar{h}$, the increment of the *pwp* (eq. (13)) can be neglected if compared with the hydrostatic one.

An additional coupled effect related to the curvature of the sliding surface arises, expecially for fine grained soils (small c_v values), if the increase of total normal stresses $\Delta\sigma_{\Delta N}$ in the saturated mass as well as an 'almost' undrained condition, that may occur during the short time interval elapsing during the curved path, are taken into account. If the elastic mechanical behaviour of the saturated mass is assumed, an additional *pwp* increase could arise and must be considered (Lambe and Withman 1969):

$$\Delta p_{w,\Delta N}(z) = C_{pw}\cdot\Delta\sigma_{\Delta N}(z) \quad (14)$$

$$\text{with } \Delta\sigma_{\Delta N}(z) = \gamma(1-S)\bar{h}\frac{v^2}{rg} + \gamma_{sat}z\frac{v^2}{rg} \quad (15)$$

C_{pw} (generally equal to 1 for saturated materials) being the *pwp* parameter for loading processes under oedometric and undrained conditions (Lambe and Whitman 1969).

At the base ($z = S\bar{h}$) of the sliding mass, eq. (13) and eq. (15) can be rewritten as follows:

$$\Delta p_{w,b,k} = \gamma_w\frac{v^2}{r(z)g}S\bar{h};\ \Delta p_{w,b,\Delta N} = C_{pw}\cdot\Delta\sigma_{b,\Delta N}$$

$\Delta\sigma_{b,\Delta N}$ being the increase of basal total normal stresses ($\Delta\sigma_{\Delta N}(z = S\bar{h})$). Under these assumptions, the resultant U of the *pwp* at the base of the sliding mass ($p_{w,b}$) should be rewritten as follows:

$$U = \left[p_{w,b,hyd} + u_b(t) + \Delta p_{w,b}\right]\cdot b \quad (16)$$

being $\Delta p_{w,b} = \Delta p_{w,b,k} + \Delta p_{w,b,\Delta N}$.

The global shear resistance force T_{max} (eq. (9)) is thus expressed as follows:

$$T_{max} = \left\{\left[mgcos\alpha + m\frac{v^2}{r}\right] - \left[p_{w,b,hyd} + u_b(t) + \Delta p_{w,b,k} + \Delta p_{w,b,\Delta N}\right]b\right\}tan\varphi' \quad (17)$$

Under the previous assumptions, eq. (10) describing the sliding of the considered block becomes:

$$\ddot{s} + \dot{s}^2 \left\{ \frac{1}{m(s(t))} \frac{dm}{ds} + \left[1 - \frac{((1-S)\gamma + (\gamma_{sat}+\gamma_w)S)\bar{h}b}{g\, m(s(t))} \right] \frac{tan\varphi'}{r(s)} \right\} - g[\sin\alpha(s) - \cos\alpha(s)\, tan\varphi'] - \left[(\gamma_w S\bar{h} \cos\alpha(s) + u_{b,0} e^{-at}) \frac{b}{m(s(t))} \right] tan\varphi' \quad (18)$$

s being the curvilinear abscissa; $\alpha(s) = \alpha_0 - s/r$ ($\alpha_0 = \alpha(s=0)$).

At time $t = 0$, the block starts its sliding along a surface sloped $\alpha=\alpha_0$, with initial speed $v=v_0$.

During motion, the mass $m(t)$ may be expressed as (Cannon and Savage 1988):

$$m(t) = m(x(t)) = m_0 + \mu'(x - x_e) \quad (19)$$

m_0 (kg) being the initial mass

$$m_0 = [(1-S)\cdot\gamma + S\cdot\gamma_{sat}]b\bar{h}/g);$$

μ' (kg/m), the erosion/deposition rate ($\mu' > 0$, erosion; $\mu' < 0$, deposition); x_e, the abscissa for which the erosion/deposition process starts; in particular, several authors (Hungr 2004) suggested: $\mu' = \mu'_e > 0$, if $\alpha(s) > \beta_e$; $\mu' = \mu'_d < 0$, if $\alpha(s) < \beta_e$, β_e being the erosion critical slope generally ranging between 8°-14°; β_e can also be evaluated through the relationship proposed by Takahashi (1991):

$$\beta_e = atan[tan\varphi'(1-2(\gamma_w/\gamma_{beb})(1/(1+(\gamma^*/\gamma_{beb}))))];$$

γ_{bed} being the unit weight of the material lying on the bed of the channel (typically, 18-20 kN/m^3); γ^* (= $(1-S)\cdot\gamma + S\cdot\gamma_{sat}$), the average (according to the factor S) unit weight of the sliding granular block.

The eq. (18) has been numerically integrated through the *Finite Difference Method* (FDM) according to the *Eulero method*.

If the integration time interval (*i.t.i*) assumes small values, the numerical solution becomes more stable, but the computation time increases; the following values $0.25s; 0.5s; 1s$ of the integration time interval have been chosen.

2.1 Admissible values for model parameters

The proposed model depends on several parameters (r, $r_{0,b}$, a or c_v, S, μ') pertaining to terrain and flow properties. Their admissible values have been evaluated by lab experiments and field observations results available in literature and providing relationships linking them to typical physical and mechanical parameters concerning the involved materials (Federico and Cesali 2017). In particular, the parameter $r_{0,b}$, if the initial basal *pwp* excess (u_{b0}) is generated by cyclic shear stresses, can be evaluated through the relationship reported in Table 1, according to the following parameters: OCR = overconsolidation ratio; A and B = parameters dependent on plasticity index PI; η = an experimental coefficient (suggested value 0.45); $\gamma_{c,max}$, the maximum shear strain, which can be assumed equal to average shear strain γ_{av}, defined in function of the maximum earthquake-induced acceleration. If u_{b0} is induced by deposition of consolidating (initially liquefied) mud granular materials, $r_{0,b}$ assumes values approximately ranging between 0.85 ÷ 0.95. The parameter a can be evaluated through the variables governing the consolidation process of the involved materials (e.g. H = the maximum drainage distance; c_v, the 1-D consolidation coefficient related to the parameters E_{ed}, oedometric modulus, and k, permeability coefficient = $k\cdot E_{ed}/\gamma_w$; γ_w, unit weight of the water, Table 1).

Table 1. Admissible values for the model parameters

Parameter	Admissible values	Relationships
$r_{0,b}$	0.85-0.95	$r_{0,b} = \eta\cdot log(\gamma_{c,max}/[A\cdot(OCR+1)+B]$
a	-	$a = \pi^2 c_v/(4H^2)$
μ'_e (=$\lvert\mu'_d\rvert$)	0 – 9 kg/m	-

The erosion (μ'_e) rate tipically ranges between $0 \div 9\cdot 10^3$ kg/m, approximately (Federico and Cesali 2017). Absolute value of μ'_d (< 0) is generally assumed equal to μ'_e (Table 1).

2.2 *Evolution of pore water pressures*

The effects of the *slope curvature* on the *pwp* (p_w) are investigated (Figs. 4, 5). The following input parameters are considered: $\varphi' = 35°$; $\bar{h} = 10$ m; $b = 50$ m; $\gamma = 14$kN/m^3; $\gamma_{sat} = 19$kN/m^3; $r_{0,b} = 0.87$; $S = 0.20$; $c_v = 0.01$ m^2/s; $\mu'_e = \mu'_d = 0$ (constant mass). The sliding surface is described according to: *i)* $\alpha_1 = 25°$; $\alpha_2 = 0°$; $L_1 = 300$ m; $r_1 = 500$ m (curved path $\widehat{PR} \cong 220$ m); *ii)* $r_2 = 3000$ m (curved path $\widehat{PQ} \cong 1300$ m), Fig. 3.

The obtained velocity and travelled distance of the fine grained materials flow and evolution of *pwp* at its base are shown in Fig. 4.

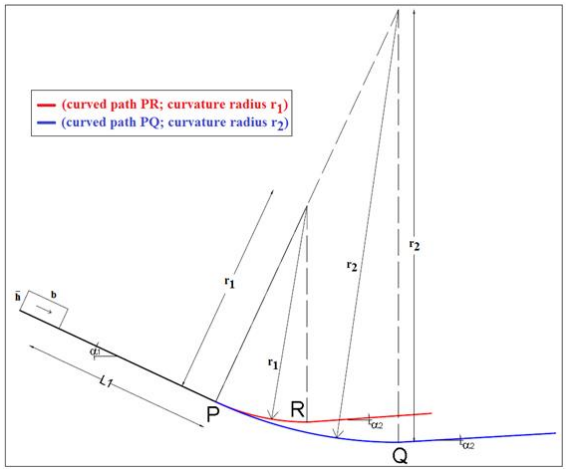

Figure 3. Schematizations of the sliding surface.

Small values of r induce a considerable increase in the basal *pwp*, especially of $\Delta p_{w,b,\Delta N}$, causing the reduction of the basal effective stresses σ' and a more rapid change of the velocity ($\Delta v/\Delta x$) of the sliding mass along the curved path; smaller values of the runout length (for $r = 500$ m) are due to a larger reduction of the slope curvature.

The role of the dissipation of the basal *pwp* excess u_b is also investigated. To this purpose, the following parameters are assigned: $\alpha_0 = 28°$; $r = 2000$m (geometrical schematization *a)*, Fig. 5); $\varphi' = 26°$; $\bar{h} = 20$ m; $S = 0.25$; $r_{0,b} = 0.88$; $\gamma = 14$kN/m^3; $\gamma_{sat} = 19$kN/m^3; $\mu'_e = \mu'_d = 0$ (constant mass).

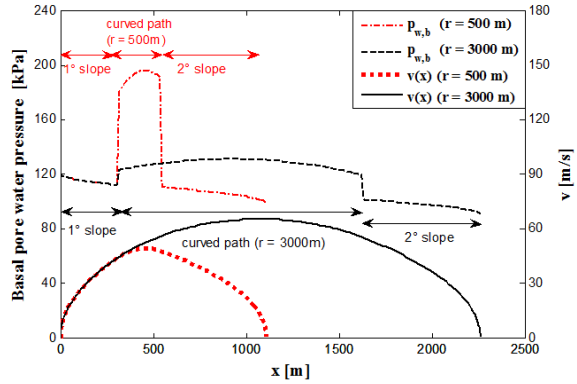

Figure 4. Basal pore water pressure and velocity (v) vs travelled distance (x), for different values of r.

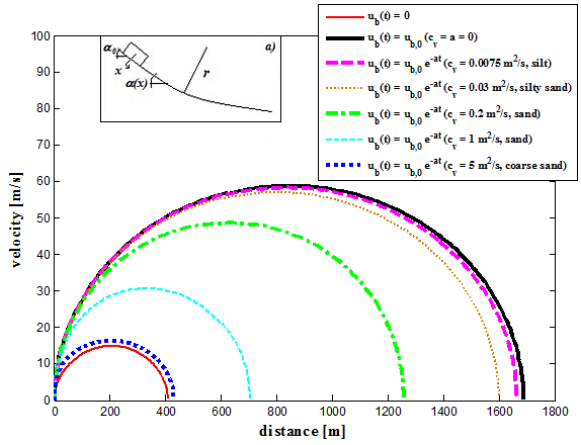

Figure 5. Velocity vs travelled distance for different values of consolidation coefficient c_v.

If c_v (and then the parameter a) decreases, the traveled distance and the maximum rate increase; for small values of c_v (e.g., silt and clayey silt), the runout length becomes almost independent on c_v and tends to the value obtained by assuming $u_b = u_{b0} = constant$ (Fig. 5).

For values of c_v characterizing a coarse sand, the runout length rapidly tends to the value obtained assuming $u_b = 0$. For silt and clay materials, the total dissipation of the basal *pwp* excess occurs for longer time than the duration of the sliding of the granular mass. For more permeable materials, the basal excess *pwp* is quickly dissipated compared with the duration of motion and it can be neglected (Fig. 6).

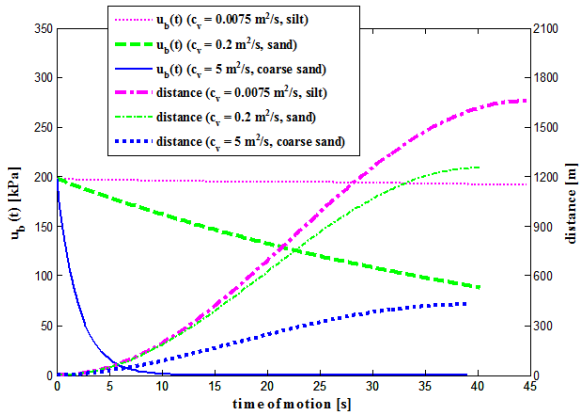

Figure 6. Basal excess pore water pressure (u_b) and travelled distance vs time, for different values of consolidation coefficient c_v.

3 APPLICATION

The large scale test performed at the USGS on August 25, 2009 (Iverson et al. 2012) is considered. The experimental apparatus is composed by a concrete channel/flume, with a rectangular (transversal) section (2 x 1.2 m), with a slope of 31° and a length of about 80 m; at the end of the flow path, a planar surface 2.4° sloped, is disposed (Fig. 7).

At the head of the flume, a mixture of sand ($d \in [0.0625 \div 2]$ mm; 33%), gravel (d ε [2 ÷ 32] mm; 66%) and water (total volume, 10 m^3) is located. Along the channel, at sections I (32 m from the gate), II (66 m from the gate) and III (80 m from the gate) (Fig. 7), sensors and transducers measure flow depth and velocity, basal *pwp* and total normal stresses. The granular flows along the channel travelled a distance of 94.5 m, reaching a maximum velocity of 6.1 m/s (Iverson et al. 2012).

To simulate the experiment, the following parameters are considered: $\alpha_1 = 31°$; $\alpha_2 = 2.4°$; $L_1 = 80$ m; $\bar{h} = 0.15$ m; $b = 30$ m; $\gamma = 18.0$ kN/m^3; $\gamma_{sat} = 20.6$ kN/m^3; $\varphi' = 39.6°$; $\mu'_e = -\mu'_d = 0$ kg/m (constant mass).

The best fitting of the values of travelled distance and maximum velocity (Fig. 8), as well as of basal interstitial pressure at section III (Fig. 9), is obtained by assuming values of S, $r_{0,b}$ and c_v (case *a)*) reasonably corresponding to the examined granular mixture.

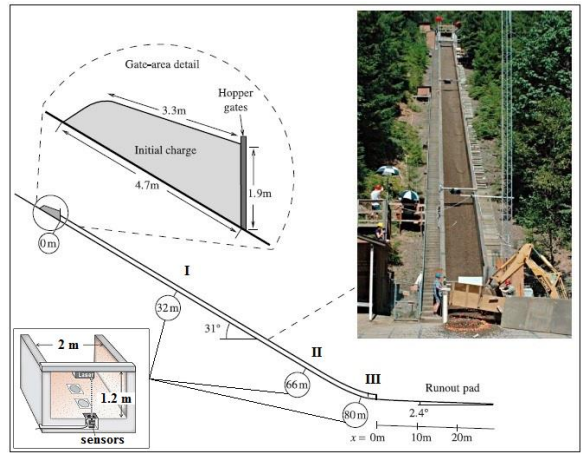

Figure 7. Experimental apparatus and location of sensors (adapted from Iverson et al. 2012).

The values S, $r_{0,b}$ e c_v are parametrically assigned: *a*) $S = 0.6$; $r_{0,b} = 0.4$; $c_v = 7.5 \cdot 10^{-4}$ m^2/s; *b*) $S = 0.8$; $r_{0,b} = 0.2$; $c_v = 5 \cdot 10^{-2}$ m^2/s; *c*) $S = 0.3$; $r_{0,b} = 0.45$; $c_v = 1 \cdot 10^{-4}$ m^2/s.

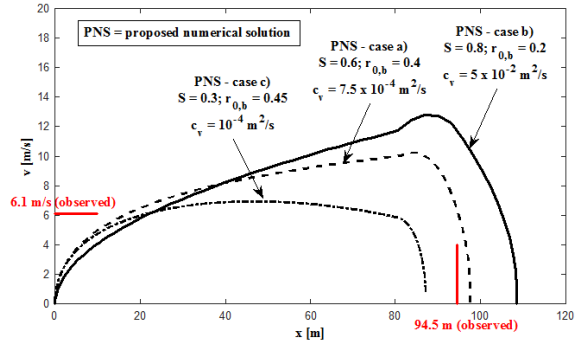

Figure 8. Proposed model: velocity vs distance.

4 CONCLUDING REMARKS

To estimate the mobility of a fine grained material flow, an analytical ("*block*") model is proposed. The dissipation of the *initial* basal excess pore water pressures (*pwp*) (these last ones induced by cyclic loads or deposition of liquefied mud masses), due to consolidation

process, as well as the *pwp* excess associated with coupled slope curvature and undrained conditions, are taken into account.

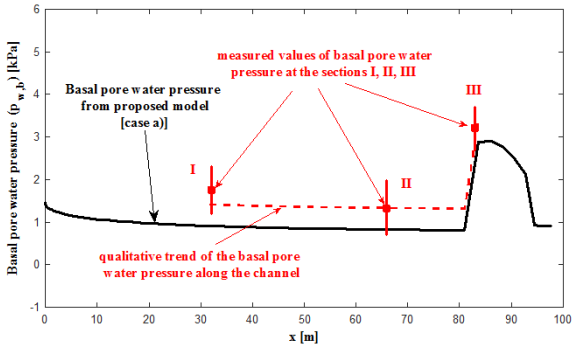

Figure 9. Proposed model: basal pore water pressure vs distance.

The evolution of *pwp* along curvilinear paths, as well as their effects on the runout, are analyzed. Finally, through a reasonable choice of physical and mechanical parameters, the proposed model allowed to interpret experimental measures of basal *pwp*, particularly its increment at the section from which the curvature of the slope bottom profile begins to change.

5 REFERENCES

Cannon, S. H., and Savage, W. Z. (1988). "A mass-change model for the estimation of debris-flow runout." *J. Geol.,* 96 (2).

Comegna, L., Picarelli, L. (2005). "The interplay between pore pressures and slope movements in fine-grained materials". *Proc., 11th IACMAG, Turin.*

Federico, F., Cesali, C. (2017). "Coupled effects of pore water pressures evolution, slope curvature and mass variation on the kinematics of rapidly sliding fine - grained materials". *IJOG (ASCE),* 10, 2017.

Hungr, O. (2004). "Flow slides and flows in granular soils". *Proc., Int. Workshop on Occurrence and Mechanisms of Flow-Like Landslidesin Natural Slopes and Earthfills, Sorrento, Picarelli ed., Kluwer Publishers.*

Hutchinson, J.N. (1986). "A sliding consolidation model for flow slides". *Can. Geotech. J.*, 23, 115-126.

Hutchinson, J.N., Bhandari, R.K. (1971). "Undrained loading, a fundamental mechanism of mudflows and other mass movements". *Géotechnique,* 21, 353–358.

Iverson, R.M., Reid, M.E., LaHusen, R.G. (1997). "Debris-flow mobilizationfrom landslides". *Annu. Rev. Earth Planet. Sci.*, 25, 85–138.

Iverson, R.M., Johnson, C.G., Kokelaar, B.P., Logan, M., LaHusen, R.G., Gray, J.M.N.T. (2012). "Grain-size segregation and levee formation in geophysical mass flows". *Journal of Geophysical Research*, vol. 117.

Lambe, T.W, Whitman, R.V. (1969). *Soil Mechanics*. *John Wiley and Sons, 553 pp.*

Miao, H., Wang, G., Yin, K., Kamai, T., Li, Y. (2014). "Mechanism of the slow-moving landslides in Jurassic red-strata in the Three Gorges Reservoir, China". *Engrg. Geol.*, 171, pp. 59-69.

Major, J.J. (2000)."Gravity-driven consolidation of granular slurries: implications for debris-flow deposition and deposit characteristics." *J. Sediment. Res*., 70(1), 64–83.

Qiao, C., Ou, G., Pan, H. (2018). "Numerical modelling of the long runout character of 2015 Shenzhen landslide with a general two-phase mass flow model". *Bulletin of Engin. Geology and the Envir., Springer, Nature*.

Siviglia, A., Cantelli, A. (2005). "Effect of bottom curvature on mudflow dynamics: theory and experiments". *Water Resources Research*, 41, 1-17.

Takahashi, T. (1991). "Debris flow", *Balkema, Rotterdam, Netherlands.*

Van Grassen, W., Cruden, D.M. (1990). "Momentum transfer in the debris of rock avalanches". *Can. Geotech. J.*, 27, pp. 623-628.